ACS Sustainable Chemistry & Engineering

pubs.acs.org/journal/ascecg

Letter

CO_2 Electroreduction to Methane at Production Rates Exceeding 100 mA/cm^2

Armin Sedighian Rasouli,[‖] Xue Wang,[‖] Joshua Wicks, Geonhui Lee, Tao Peng, Fengwang Li, Christopher McCallum, Cao-Thang Dinh, Alexander H. Ip, David Sinton, and Edward H. Sargent*

Cite This: https://dx.doi.org/10.1021/acssuschemeng.0c03453

Read Online

ACCESS | Metrics & More | Article Recommendations | Supporting Information

ABSTRACT: The electrochemical reduction of CO_2 to methane is a promising method to store intermittent renewable energy. Previous research reporting high methane selectivity has relied on H-cells, and total current densities have therefore resided below 50 mA/cm^2, insufficient for industrial applications. Here, we increase the methane production rate by modifying the system so that it functions efficiently in a flow cell configuration. We investigate the impact of the local environment on methane selectivity in flow cells by tuning the choice of electrolyte cation, catalyst thickness, and local pH. We achieve a methane selectivity of 48% ± 4% with a partial current density of 120 ± 10 mA/cm^2, representing a cathodic energy efficiency of 23%. We showcase a stable operation for 14 h.

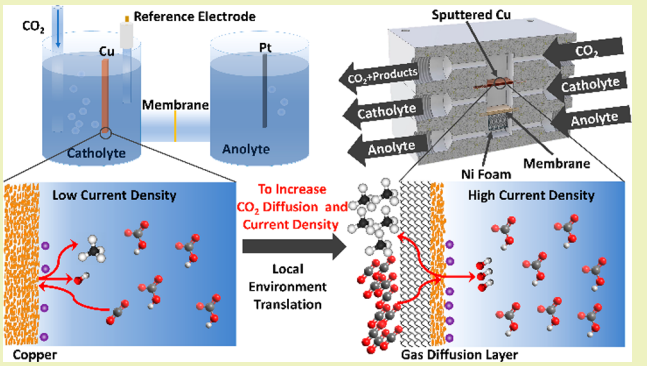

KEYWORDS: *CO_2 reduction reaction, Flow cell, Methane, Local environment, Electrolyte cation, Catalyst thickness, Local pH*

Downloaded via UNIV OF TORONTO on September 21, 2020 at 16:19:32 (UTC).
See https://pubs.acs.org/sharingguidelines for options on how to legitimately share published articles.

INTRODUCTION

The electrochemical CO_2 reduction reaction (CO_2RR) to chemicals and fuels is a promising method to store renewable electricity.[1,2] Different monocarbon and multicarbon products have been reported in CO_2RR.[3−7] High Faradaic efficiencies (FEs) toward a specific product with high production rates have been reported for ethylene,[3,4] ethanol,[5] CO,[6] and formate.[7] Among the products of CO_2RR, renewable methane—a carbon-neutral fuel alternative to fossil fuels—is of interest because the infrastructure to store, transport, and use methane as a fuel is already well established.[8]

Prior CO_2-to-methane electrochemical production research has relied on the H-cell configuration and suffers therefore from a low methane production rate,[9−11] with current densities under 50 mA/cm^2,[12−15] values that reside below industrially applicable levels.[16−18] In H-cells, the reaction rate of CO_2RR is restricted by the limited mass transfer of CO_2, as only dissolved CO_2 in the aqueous catholyte can be used as the reactant.[16] Technoeconomic studies show that to reach a compelling large-scale CO_2RR system, high selectivity, current density, and energy efficiency will be required.[17] Capital and product separation costs will decrease with high selectivity and current density.[17]

A flow cell system offers a route to overcome the reactant mass transfer limit and provide a triple-phase interface allowing CO_2 to contact the catalyst−electrolyte interface and thus to meet the requirement of high current density.[13] However, since a significant increase in current density results in a changed local reaction environment, the CO_2RR product distribution in H-cells is different from that in flow cells.[16]

Here, with the goal of achieving a high methane selectivity with a high production rate, we investigate the effects of alkali metal cations and the thickness of the catalyst layer in the flow cell during CO_2RR. We model the local pH in both H-cell and flow cell configurations and experimentally identify operating parameters that translate the local pH of the H-cell into the flow cell configuration. Levering this understanding, we transfer the high methane selectivity in H-cells to the flow cell configuration. We achieve a methane Faradaic efficiency (FE) of (48 ± 4)% with a methane partial current density of 120 ± 10 mA/cm^2 and a cathodic energy efficiency ($EE_{cathodic}$) of 23%, as well as a stable operation for 14 h.

RESULTS AND DISCUSSION

To investigate the different local reaction environments in H-cell and flow-cell configurations, we first performed CO_2RR in H-cells using an electropolished Cu sheet as the cathode catalyst (Figure 1). To query the effect of cations on CO_2RR selectivity toward methane in the H-cell configuration (Figure

Received: May 9, 2020
Revised: August 10, 2020
Published: September 14, 2020

© XXXX American Chemical Society

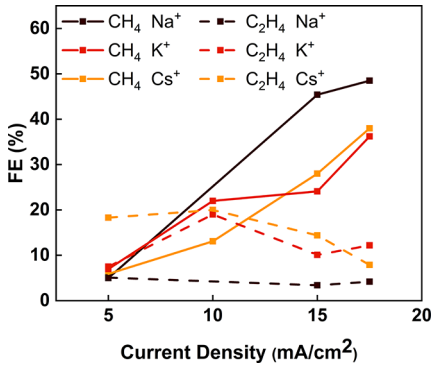

Figure 1. CH_4 and C_2H_4 FE on electropolished Cu sheet in an H-cell configuration with $KHCO_3$, $NaHCO_3$, and $CsHCO_3$ electrolytes.

S1), we used $KHCO_3$ and $NaHCO_3$ as electrolytes. The selectivity toward methane in 0.1 M $NaHCO_3$ is higher than that in 0.1 M $KHCO_3$ (Figure 1), in agreement with previous reports.[14,15] The *CO protonation to *CHO is the potential-determining step for CH_4 formation.[19,20] Compared to Na^+, K^+ stabilizes the *CO intermediate, leading to an increase in the *CO protonation energy and a decrease in methane selectivity.[14,19] The Cs^+ cations have previously been seen to promote ethylene selectivity and suppress HER by increasing CO_2RR activity (Figure 1 and Figure S2).[19] Though the methane FE in 0.1 M $NaHCO_3$ is 49%, the methane partial current density is as low as 9 mA/cm^2, significantly hindered by the limited mass transport of CO_2.

We then performed CO_2RR using 500 nm thick sputtered Cu (Figure 2b and c and Figure S3) in a flow cell configuration (Figure 2a) using 1 M $KHCO_3$, 1 M $NaHCO_3$, and 1 M $CsHCO_3$ as electrolytes under a 60% dilute CO_2 gas stream. We have previously shown that methane selectivity can be improved by using a dilute CO_2 gas stream,[21] and we use this approach in the flow cell studies herein. When the current density is lower than 200 mA/cm^2, methane selectivity in a $NaHCO_3$ electrolyte is higher than that in the $KHCO_3$ electrolyte (Figure 2b), consistent with the H-cell trend (Figure 1). The limiting current density in an anion exchange membrane and electrolyte depends on the ionic species transport properties.[22−24] The lower conductivity and diffusion coefficient of Na^+ ions versus K^+ ions[25] limit the maximum operating current density to 225 mA/cm^2 in the 1 M $NaHCO_3$ electrolyte.[25] A further increase in current density to 250 mA/cm^2 in $KHCO_3$ results in a methane FE of 26%, which is due to the more negative potential on the cathode leading to a shift in the product distribution toward methane. The superior performance in $KHCO_3$ compared to $NaHCO_3$ at high current densities is attributed to a lower electrolyte resistance,[25] a more negative surface charge density on the catalyst, and a higher buffering capacity of K^+, which favors CO_2RR to methane.[3,19] $CsHCO_3$ promotes C_2H_4 selectivity with a low methane selectivity compared to $KHCO_3$ since *CO

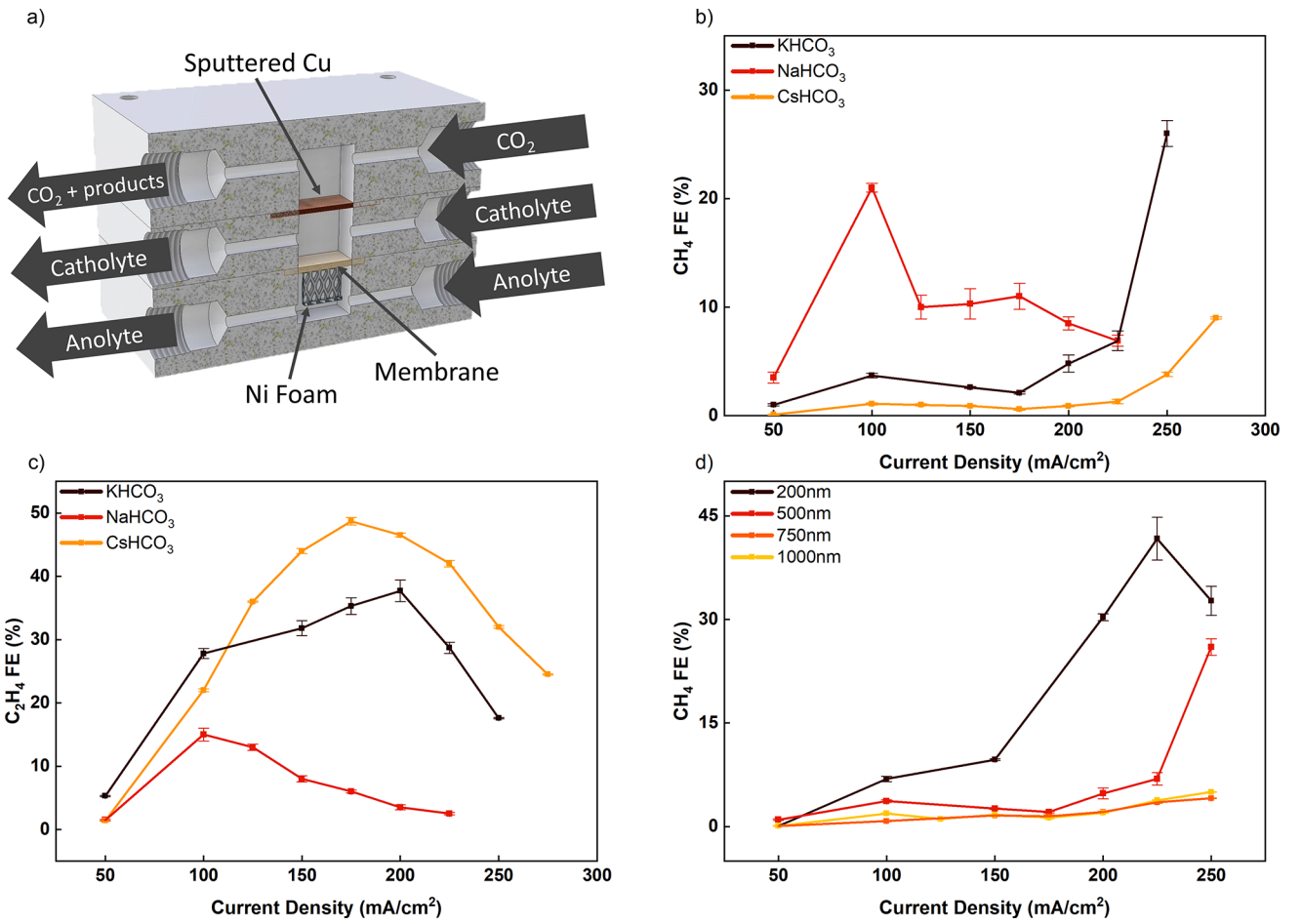

Figure 2. (a) Schematic of the flow cell configuration. (b) CH_4 FE and (c) C_2H_4 FE on 500 nm sputtered Cu using 1 M $XHCO_3$ (X: Na, K, Cs) in the flow cell. (d) CH_4 FE from sputtered Cu with different thicknesses using 1 M $KHCO_3$ in the flow cell.

https://dx.doi.org/10.1021/acssuschemeng.0c03453
ACS Sustainable Chem. Eng. XXXX, XXX, XXX−XXX

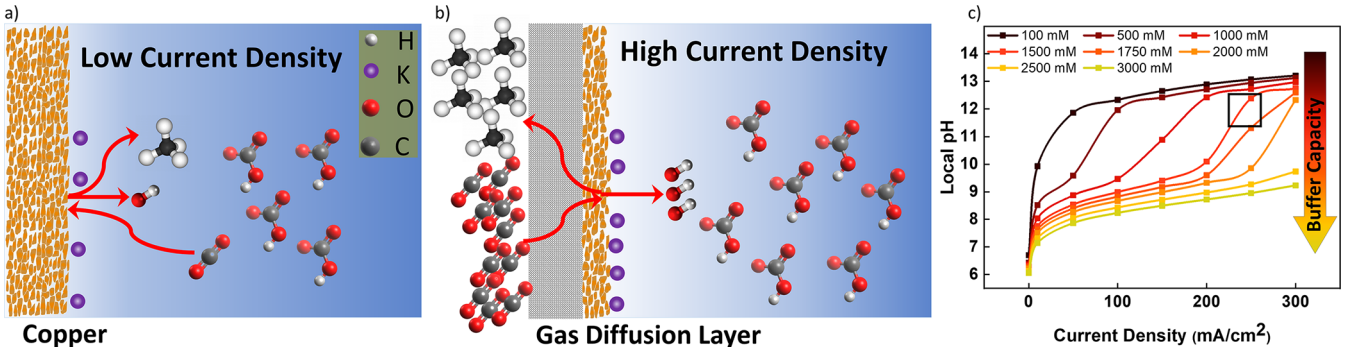

Figure 3. Cathodic half-cell configurations in H-cell (a) and flow cell (b), illustrating higher CO_2 diffusion and concentration at the Cu surface in the flow cell. The legend in panel (a) also applies to panel (b). (c) Local pH modeling on the cathode surface during CO_2RR in the flow cell configuration with different HCO_3^- concentrations and current densities (the box is the region with the highest methane selectivity in the flow cell configuration).

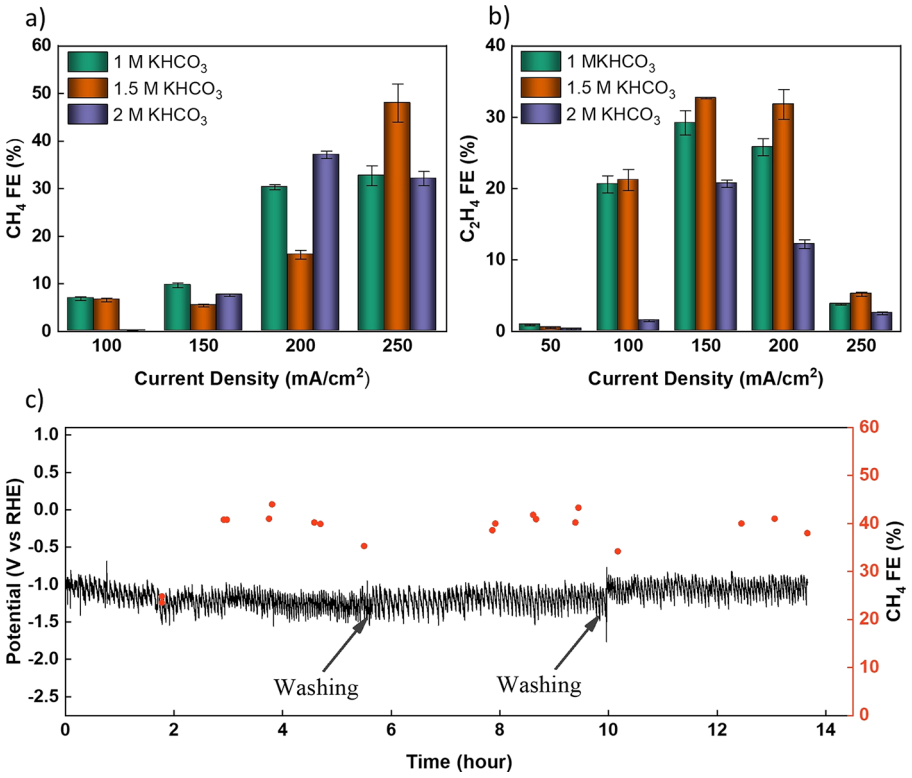

Figure 4. (a) CH_4 FE and (b) C_2H_4 FE on 200 nm sputtered Cu with different $KHCO_3$ concentrations in flow cells. (c) 14 h study of 200 nm sputtered Cu by applying 250 mA/cm^2 with a 1.5 M $KHCO_3$ electrolyte in a flow cell.

stabilization in $CsHCO_3$ is higher than that in $KHCO_3$, thus preventing the protonation of *CO and instead encouraging C−C coupling (Figure 2c).[19] $KHCO_3$ and $CsHCO_3$ electrolytes with larger cations compared to $NaHCO_3$ also suppressed H_2 evolution; the K^+/Cs^+ ion-induced field stabilize CO_2RR intermediates on catalyst surfaces,[19] consistent with results in H-cells (Figure 1 and Figure S2). On the basis of the results above, we used the $KHCO_3$ electrolyte for further optimization.

We investigated CO_2RR performance on a series of sputtered Cu catalysts with thicknesses of 200, 500, 750, and 1000 nm in the flow cell (Figure 2d and Figure S4) as catalyst layer thickness has been reported to affect the product distribution when targeting other CO_2RR products in different electrolytes.[3] We found that 200 nm sputtered Cu (Figures S5 and S6) showed the highest methane FE of 42% (Figure 2d). The ethylene and hydrogen FEs on sputtered Cu with various thicknesses illustrate a selectivity shift from methane to ethylene with increasing catalyst layer thickness (Figure 2d and Figure S4a). Since the sputtered Cu is hydrophilic, the thickness of the catalyst layer affects the CO_2 availability on the catalyst surface, thereby changing the product distribution.[3] We found that the electrochemical surface area (ECSA) decreases with the thickness (Figure S7), and thus the increase in ECSA-normalized current density results in a higher local pH in thicker samples and tends to promote C_2H_4 selectivity (Figure S8 and Table S1).[3,26]

The local pH plays an essential role in *CO protonation—the potential-determining step for methane production[27]—and decreasing local pH favors methane production over C_2 products (Figure S9).[3,26−28]

https://dx.doi.org/10.1021/acssuschemeng.0c03453
ACS Sustainable Chem. Eng. XXXX, XXX, XXX−XXX

We used COMSOL Multiphysics modeling to explore further local pH under different current densities for the flow cell versus the H-cell (Figure 3 and Figure S10). Figure 3a and b show the cathodic half-cell configurations in the H-cell and flow cell, which indicates the improvement of CO_2 availability—CO_2 concentration at the surface of Cu—at high current densities in the flow cell compared to that of in the H-cell (Figure 3a and b). The simulation results in the H-cell show that the local pH—where methane FE is 49% (Figure 1) with a total current density of 17.5 mA/cm^2—is 11.5 ± 0.5 (Figure S10). Figure 3c exhibits the local pH under different current densities and concentrations of the $KHCO_3$ electrolyte in a flow cell. In flow cells, the local pH is tunable by using different electrolyte concentrations and applying different current densities.

We then evaluated CO_2RR performance experimentally on 200 nm sputtered Cu at different concentrations of $KHCO_3$ in flow cells. We compared the product distribution as a function of different current densities and different concentrations of $KHCO_3$ (Figure 4a and b and Figures S11 and S12). The highest methane FE of 48% ± 4% is obtained in 1.5 M $KHCO_3$ at 250 mA/cm^2 (Figure 4a) and has a total liquid product FE below 12% (Table S2), corresponding to a local pH of 12 ± 0.4 (Figure 3c); this represents a $EE_{cathodic}$ of 23% at the applied potential of −0.98 V vs reversible hydrogen electrode (RHE) corrected by ohmic loss. This methane FE of 48% ± 4% in the flow cell is comparable to the highest H-cell methane FE (49%), while the methane partial current density is as high as 120 ± 10 mA/cm^2. The local pH values that provides the highest methane FE in the flow cell and the H-cell are similar, confirming the significance of local pH on the CO_2RR product distribution. We observed that the $FE_{Methane}/FE_{Hydrogen}$ increases with the increase of local pH, further confirming that local pH improves methane selectivity (Figure S13). Gas chromatography−mass spectrometry (GC-MS) analyses demonstrated that CH_4 was produced via CO_2RR rather than from contaminants (Figure S14). Table S3 shows a performance comparison between this work and prior reports at technoeconomically relevant current densities.

On the basis of the optimized conditions above for methane production, we investigated the stability of the 200 nm sputtered Cu catalyst using a 1.5 M $KHCO_3$ electrolyte in a flow cell (Figure 4c). In this experiment, we used a humidified CO_2 gas stream and washed the catalyst regularly to mitigate K_2CO_3 and $KHCO_3$ salt formation and remove the salts between the Cu and polytetrafluoroethylene (PTFE) boundary, which can hinder CO_2 availability.[29] We achieved 14 h of stable CO_2-to-methane electrolysis with a methane FE over 40% under a constant total current density of 250 mA/cm^2.

CONCLUSIONS

In this work, we investigated the effect of the local reaction environment on CO_2RR to methane at technoeconomically appealing current densities. Our experiments in the H-cell configuration show a methane FE of 49% with a methane partial current density of 9 mA/cm^2 using 0.1 M $NaHCO_3$ as the electrolyte. To improve the methane production rate, we transferred the reaction from an H-cell to flow cell. In the investigation of electrolytes with different cations, $KHCO_3$ favors the increase of methane selectivity under high current density (250 mA/cm^2). We performed CO_2RR on Cu catalysts with different thicknesses and observed that sputtered Cu of a 200 nm thickness showed the highest selectivity toward methane. We found, by modeling local pH in flow cells and H-cells, that when matching the local pH in a flow cell to that of the highest H-cell methane FE, we achieved the highest flow cell methane selectivity on a 200 nm sputtered Cu catalyst: methane FE of 48% ± 4% with a partial current density of 120 ± 10 mA/cm^2, as well as an $EE_{cathodic}$ of 23% under a 1.5 M $KHCO_3$ electrolyte in the flow cell. Furthermore, this optimized CO_2-to-methane system can be operated for 14 h at an applied current density of 250 mA/cm^2 while maintaining a methane FE over 40%. This work enables the direct conversion of CO_2 feedstocks to renewable methane with high selectivity at an industrially relevant production rate.

ASSOCIATED CONTENT

Supporting Information

The Supporting Information is available free of charge at https://pubs.acs.org/doi/10.1021/acssuschemeng.0c03453.

Experimental details, structure characterization, electrochemical measurement details, cathode washing procedure, COMSOL Multiphysics modeling details, H-cell configuration schematic view, SEM images, XRD pattern, ECSA measurements, reaction scheme, modeling scheme, H_2 FE, potential versus current density, $FE_{Methane}/FE_{Hydrogen}$ versus local pH, $^{13}CO_2$ control experiments, total product distribution, and performance comparison (PDF)

AUTHOR INFORMATION

Corresponding Author

Edward H. Sargent − *Department of Electrical and Computer Engineering, University of Toronto, Toronto, Ontario M5S 1A4, Canada;* orcid.org/0000-0003-0396-6495; Email: ted.sargent@utoronto.ca

Authors

Armin Sedighian Rasouli − *Department of Electrical and Computer Engineering, University of Toronto, Toronto, Ontario M5S 1A4, Canada;* orcid.org/0000-0002-0807-9468

Xue Wang − *Department of Electrical and Computer Engineering, University of Toronto, Toronto, Ontario M5S 1A4, Canada;* orcid.org/0000-0002-6298-1858

Joshua Wicks − *Department of Electrical and Computer Engineering, University of Toronto, Toronto, Ontario M5S 1A4, Canada*

Geonhui Lee − *Department of Electrical and Computer Engineering, University of Toronto, Toronto, Ontario M5S 1A4, Canada*

Tao Peng − *Department of Electrical and Computer Engineering, University of Toronto, Toronto, Ontario M5S 1A4, Canada;* orcid.org/0000-0001-8517-5368

Fengwang Li − *Department of Electrical and Computer Engineering, University of Toronto, Toronto, Ontario M5S 1A4, Canada;* orcid.org/0000-0003-1531-2966

Christopher McCallum − *Department of Mechanical and Industrial Engineering, University of Toronto, Toronto, Ontario M5S 3G8, Canada;* orcid.org/0000-0001-6079-746X

Cao-Thang Dinh − *Department of Electrical and Computer Engineering, University of Toronto, Toronto, Ontario M5S 1A4, Canada; Department of Chemical Engineering, Queen's University, Kingston, Ontario K7L 3N6, Canada;* orcid.org/0000-0001-9641-9815

https://dx.doi.org/10.1021/acssuschemeng.0c03453
ACS Sustainable Chem. Eng. XXXX, XXX, XXX−XXX

Alexander H. Ip − *Department of Electrical and Computer Engineering, University of Toronto, Toronto, Ontario M5S 1A4, Canada*

David Sinton − *Department of Mechanical and Industrial Engineering, University of Toronto, Toronto, Ontario M5S 3G8, Canada;* orcid.org/0000-0003-2714-6408

Complete contact information is available at: https://pubs.acs.org/10.1021/acssuschemeng.0c03453

Author Contributions

‖A. Sedighian Rasouli and X. Wang contributed equally. The manuscript was written through contributions from all authors.

Notes

The authors declare no competing financial interest.

■ ACKNOWLEDGMENTS

This work was supported by the Natural Gas Innovation Fund, the Natural Sciences and Engineering Research Council (NSERC) of Canada, the Natural Resources Canada Clean Growth Program, and the Ontario Research Fund − Research Excellence program. A.S.R. acknowledges CMC Microsystems.

■ REFERENCES

(1) Centi, G.; Perathoner, S. Opportunities and Prospects in the Chemical Recycling of Carbon Dioxide to Fuels. *Catal. Today* **2009**, *148* (3), 191−205.

(2) Kondratenko, E. V.; Mul, G.; Baltrusaitis, J.; Larrazábal, G. O.; Pérez-Ramírez, J. Status and Perspectives of CO_2 Conversion into Fuels and Chemicals by Catalytic, Photocatalytic and Electrocatalytic Processes. *Energy Environ. Sci.* **2013**, *6* (11), 3112−3135.

(3) Dinh, C.-T.; Burdyny, T.; Kibria, M. G.; Seifitokaldani, A.; Gabardo, C. M.; Garcia de Arquer, F. P.; Kiani, A.; Edwards, J. P.; De Luna, P.; Bushuyev, O. S.; Zou, C.; Quintero-Bermudez, R.; Pang, Y.; Sinton, D.; Sargent, E. H. CO_2 Electroreduction to Ethylene via Hydroxide-Mediated Copper Catalysis at an Abrupt Interface. *Science* **2018**, *360* (6390), 783−787.

(4) Li, F.; Thevenon, A.; Rosas-Hernández, A.; Wang, Z.; Li, Y.; Gabardo, C. M.; Ozden, A.; Dinh, C. T.; Li, J.; Wang, Y.; Edwards, J. P.; Xu, Y.; McCallum, C.; Tao, L.; Liang, Z.-Q.; Luo, M.; Wang, X.; Li, H.; O'Brien, C. P.; Tan, C.-S.; Nam, D.-H.; Quintero-Bermudez, R.; Zhuang, T.-T.; Li, Y. C.; Han, Z.; Britt, R. D.; Sinton, D.; Agapie, T.; Peters, J. C.; Sargent, E. H. Molecular Tuning of CO_2-to-Ethylene Conversion. *Nature* **2020**, *577*, 509−513.

(5) Li, Y. C.; Wang, Z.; Yuan, T.; Nam, D.-H.; Luo, M.; Wicks, J.; Chen, B.; Li, J.; Li, F.; de Arquer, F. P. G.; Wang, Y.; Dinh, C.-T.; Voznyy, O.; Sinton, D.; Sargent, E. H. Binding Site Diversity Promotes CO_2 Electroreduction to Ethanol. *J. Am. Chem. Soc.* **2019**, *141* (21), 8584−8591.

(6) Ren, S.; Joulié, D.; Salvatore, D.; Torbensen, K.; Wang, M.; Robert, M.; Berlinguette, C. P. Molecular Electrocatalysts Can Mediate Fast, Selective CO_2 Reduction in a Flow Cell. *Science* **2019**, *365* (6451), 367−369.

(7) Xia, C.; Zhu, P.; Jiang, Q.; Pan, Y.; Liang, W.; Stavitski, E.; Alshareef, H. N.; Wang, H. Continuous Production of Pure Liquid Fuel Solutions via Electrocatalytic CO_2 Reduction Using Solid-Electrolyte Devices. *Nat. Energy* **2019**, *4* (9), 776−785.

(8) Vogt, C.; Monai, M.; Kramer, G. J.; Weckhuysen, B. M. The Renaissance of the Sabatier Reaction and Its Applications on Earth and in Space. *Nat. Catal.* **2019**, *2* (3), 188−197.

(9) Ren, D.; Fong, J.; Yeo, B. S. The Effects of Currents and Potentials on the Selectivities of Copper toward Carbon Dioxide Electroreduction. *Nat. Commun.* **2018**, *9* (1), 925.

(10) Hashiba, H.; Sato, H. K.; Yotsuhashi, S.; Fujii, K.; Sugiyama, M.; Nakano, Y. A Broad Parameter Range for Selective Methane Production with Bicarbonate Solution in Electrochemical CO_2 Reduction. *Sustain. Energy Fuels* **2017**, *1* (8), 1734−1739.

(11) Ma, S.; Sadakiyo, M.; Heima, M.; Luo, R.; Haasch, R. T.; Gold, J. I.; Yamauchi, M.; Kenis, P. J. A. Electroreduction of Carbon Dioxide to Hydrocarbons Using Bimetallic Cu-Pd Catalysts with Different Mixing Patterns. *J. Am. Chem. Soc.* **2017**, *139* (1), 47−50.

(12) Reske, R.; Mistry, H.; Behafarid, F.; Roldan Cuenya, B.; Strasser, P. Particle Size Effects in the Catalytic Electroreduction of CO_2 on Cu Nanoparticles. *J. Am. Chem. Soc.* **2014**, *136* (19), 6978−6986.

(13) Weng, Z.; Zhang, X.; Wu, Y.; Huo, S.; Jiang, J.; Liu, W.; He, G.; Liang, Y.; Wang, H. Self-Cleaning Catalyst Electrodes for Stabilized CO_2 Reduction to Hydrocarbons. *Angew. Chem., Int. Ed.* **2017**, *56* (42), 13135−13139.

(14) Kaneco, S.; Hiei, N.; Xing, Y.; Katsumata, H.; Ohnishi, H.; Suzuki, T.; Ohta, K. Electrochemical Conversion of Carbon Dioxide to Methane in Aqueous $NaHCO_3$ Solution at Less than 273 K. *Electrochim. Acta* **2002**, *48* (1), 51−55.

(15) Kibria, M. G.; Dinh, C.-T.; Seifitokaldani, A.; De Luna, P.; Burdyny, T.; Quintero-Bermudez, R.; Ross, M. B.; Bushuyev, O. S.; Garcia de Arquer, F. P.; Yang, P.; Sinton, D.; Sargent, E. H. A Surface Reconstruction Route to High Productivity and Selectivity in CO_2 Electroreduction toward C_{2+} Hydrocarbons. *Adv. Mater.* **2018**, *30* (49), 1804867.

(16) Burdyny, T.; Smith, W. A. CO_2 Reduction on Gas-Diffusion Electrodes and Why Catalytic Performance Must Be Assessed at Commercially-Relevant Conditions. *Energy Environ. Sci.* **2019**, *12* (5), 1442−1453.

(17) Jouny, M.; Luc, W.; Jiao, F. General Techno-Economic Analysis of CO_2 Electrolysis Systems. *Ind. Eng. Chem. Res.* **2018**, *57* (6), 2165−2177.

(18) Gabardo, C. M.; Seifitokaldani, A.; Edwards, J. P.; Dinh, C.-T.; Burdyny, T.; Kibria, M. G.; O'Brien, C. P.; Sargent, E. H.; Sinton, D. Combined High Alkalinity and Pressurization Enable Efficient CO_2 Electroreduction to CO. *Energy Environ. Sci.* **2018**, *11* (9), 2531−2539.

(19) Resasco, J.; Chen, L. D.; Clark, E.; Tsai, C.; Hahn, C.; Jaramillo, T. F.; Chan, K.; Bell, A. T. Promoter Effects of Alkali Metal Cations on the Electrochemical Reduction of Carbon Dioxide. *J. Am. Chem. Soc.* **2017**, *139* (32), 11277−11287.

(20) Liu, X.; Xiao, J.; Peng, H.; Hong, X.; Chan, K.; Nørskov, J. K. Understanding Trends in Electrochemical Carbon Dioxide Reduction Rates. *Nat. Commun.* **2017**, *8* (1), 1−7.

(21) Wang, X.; Xu, A.; Li, F.; Hung, S.-F.; Nam, D.-H.; Gabardo, C. M.; Wang, Z.; Xu, Y.; Ozden, A.; Rasouli, A. S.; Ip, A. H.; Sinton, D.; Sargent, E. H. Efficient Methane Electrosynthesis Enabled by Tuning Local CO_2 Availability. *J. Am. Chem. Soc.* **2020**, *142* (7), 3525−3531.

(22) Lee, H.-J.; Strathmann, H.; Moon, S.-H. Determination of the Limiting Current Density in Electrodialysis Desalination as an Empirical Function of Linear Velocity. *Desalination* **2006**, *190* (1), 43−50.

(23) Tanaka, Y. Chapter 11 Limiting Current Density. In *Ion Exchange Membranes*; Tanaka, Y., Ed.; Membrane Science and Technology Series; Elsevier, 2007; Vol. *12*, pp 245−270. DOI: 10.1016/S0927-5193(07)12011-8.

(24) Hicks, M. T.; Fedkiw, P. S. Effects of Supporting Electrolyte on the Mass-Transfer Limited Current for Coupled Chemical-Electrochemical Reactions. *J. Electroanal. Chem.* **1997**, *424* (1), 75−92.

(25) Salazar-Villalpando, M. D. Effect of Electrolyte on the Electrochemical Reduction of CO_2. *ECS Trans.* **2010**, *33* (27), 77−88.

(26) Liu, X.; Schlexer, P.; Xiao, J.; Ji, Y.; Wang, L.; Sandberg, R. B.; Tang, M.; Brown, K. S.; Peng, H.; Ringe, S.; Hahn, C.; Jaramillo, T. F.; Nørskov, J. K.; Chan, K. PH Effects on the Electrochemical Reduction of CO_2 towards C_2 Products on Stepped Copper. *Nat. Commun.* **2019**, *10* (1), 32.

(27) Cheng, M.-J.; Clark, E. L.; Pham, H. H.; Bell, A. T.; Head-Gordon, M. Quantum Mechanical Screening of Single-Atom Bimetallic Alloys for the Selective Reduction of CO_2 to C_1 Hydrocarbons. *ACS Catal.* **2016**, *6* (11), 7769−7777.

(28) Montoya, J. H.; Shi, C.; Chan, K.; Nørskov, J. K. Theoretical Insights into a CO Dimerization Mechanism in CO_2 Electroreduction. *J. Phys. Chem. Lett.* **2015**, *6* (11), 2032−2037.
(29) Nwabara, U. O.; Cofell, E. R.; Verma, S.; Negro, E.; Kenis, P. J. A. Durable Cathodes and Electrolyzers for the Efficient Aqueous Electrochemical Reduction of CO_2. *ChemSusChem* **2020**, *13*, 855.

https://dx.doi.org/10.1021/acssuschemeng.0c03453
ACS Sustainable Chem. Eng. XXXX, XXX, XXX−XXX